Volume and Free Energy of Folding for Troponin C C-Domain: Linkage to Ion Binding and N-Domain Interaction[†,‡]

Cristiane Barbosa Rocha,[§,#] Marisa C. Suarez,[||,#] Aimee Yu,[⊥,⊗] Lance Ballard,[⊥,○] Martha M. Sorenson,[§] Débora Foguel,[*,§] and Jerson L. Silva[*,§]

Instituto de Bioquímica Médica, Centro Nacional de Ressonância Magnética Nuclear Jiri Jonas, Universidade Federal do Rio de Janeiro 21941-590, Rio de Janeiro, RJ, Brazil, UEZO−Centro Universitário Estadual da Zona Oeste, R. Manoel Caldeira de Alvarenga 1203, Rio de Janeiro, RJ, Brazil, and School of Chemical Sciences, University of Illinois, Urbana, Illinois 61801

Received October 13, 2007; Revised Manuscript Received February 26, 2008

ABSTRACT: Troponin C (TnC) is an 18-kDa acidic protein of the EF-hand family that serves as the trigger for muscle contraction. In this study, we investigated the thermodynamic stability of the C-domain of TnC in all its occupancy states (apo, Mg^{2+}-, and Ca^{2+}-bound states) using a fluorescent mutant with Phe 105 replaced by Trp (F105W/C-domain, residues 88–162) and ^1H NMR spectroscopy. High hydrostatic pressure was employed as a perturbing agent, in combination with urea or without it. On the basis of changes in Trp emission, the C-domain apo state was denatured by pressure (in the range of 1−1000 bar) in the absence of urea. The fluorescence data were corroborated by following the changes in the ^1H NMR signal of Histidine 128. Addition of Ca^{2+} or Mg^{2+} increased the C-domain stability so that complete denaturation was attained only by the combined use of high hydrostatic pressure and either 7−8 M or 1.5−2 M urea, respectively. The ^1H NMR spectra in the presence of Ca^{2+} was typical of a highly structured protein and allowed us to follow the changes in the local environment of several amino-acid residues as a function of pressure at 4 M Urea. Different residues presented different volume changes, but those that are in the hydrophobic core portrayed values very similar to that obtained for tryptophan 105 as measured by fluorescence, indicating that it is indeed a good probe for the overall tertiary structure. From these experiments, we calculated the thermodynamic parameters ($\Delta G°_{atm}$ and ΔV) that govern the folding of the C-domain in all its possible physiological states and constructed a thermodynamic cycle. Furthermore, a comparison of the volume and free-energy changes of folding of isolated C-domain with those of intact TnC (F105W) revealed that the N-domain has little effect on the structure of the C-domain, even in the presence of Ca^{2+}. The volume and free-energy diagrams reveal a landscape of different conformations from the less structured, denatured apo form to the highly structured, Ca^{2+}-bound form. The large change in folding free energy of the C-domain that takes place when Ca^{2+} binds may explain the much higher Ca^{2+} affinity of sites III and IV, 2 orders of magnitude higher than the affinity of sites I and II.

Troponin C (TnC[1]) is a member of the EF-hand family, which comprises several proteins that share a common helix–loop–helix motif responsible for Ca^{2+} binding (*1, 2*). TnC is a subunit of the troponin complex (TnC, TnI and TnT), which, in concert with tropomyosin, modulates the cyclic interaction between myosin and actin during muscle contraction (for reviews, see *3*−*6*). Its structure, revealed by crystal diffraction studies, showed that TnC is organized into two globular domains, N and C, separated by a rigid central helix (*7–10*). Each domain has two ion-binding sites: sites I and II in the N-domain display specificity and a relatively low affinity for Ca^{2+} ($K_{a[Ca]} \cong 10^5\ M^{-1}$); sites III and IV in the C-domain bind Mg^{2+} ($K_{a[Mg]} \cong 10^3\ M^{-1}$) or Ca^{2+} ($K_{a[Ca]} \cong 10^7\ M^{-1}$). In addition to the two classes of sites, there is evidence for an additional class, the weak sites, that bind Mg^{2+} as well as Ca^{2+} with very low affinity ($K_{a[Ca, Mg]} \sim 10$ (*2*) $-10^3\ M^{-1}$) (*11–15*). Recently, we observed that Ca^{2+} or Mg^{2+} binding to weak sites of TnC C-domain induces exposure of a large hydrophobic surface that leads to loss of TnC from the thin filament (*15*).

There is strong evidence supporting the idea that the N-domain has a regulatory role: it triggers muscle contraction and relaxation upon Ca^{2+} binding and release (*3, 16*). On the basis of the similarities in the amino-acid sequences of the N- and C-domains and by assuming that the structure of the Ca^{2+}-

[†] This work was supported by grants from Conselho Nacional de Desenvolvimento Científico e Tecnológico (CNPq), Millenium Institute for Structural Biology in Biomedicine and Biotechnology (CNPq Millenium Program), Fundação Carlos Chagas Filho de Amparo à Pesquisa do Estado do Rio de Janeiro (FAPERJ) and Financiadora de Estudos e Projetos (FINEP) of Brazil to D.F., J.L.S., and M.M.S.

[‡] This work is dedicated to Leopoldo de Meis in commemoration of his 70th birthday.

* To whom correspondence should be addressed. Phone: 5521 2543-4357. Fax: 5521 2270-8647. E-mail: jerson@bioqmed.ufrj.br (J.L.S.); foguel@bioqmed.ufrj.br (D.F.).

[§] Universidade Federal do Rio de Janeiro.

[||] UEZO−Centro Universitário Estadual da Zona Oeste.

[⊥] University of Illinois.

[#] C.B.R. and M.C.S. contributed equally to this study.

[⊗] Current address: The Mayo Clinic, Rochester, MN 55901.

[○] Current address: Bruker BioSpin, Billerica, MA 01821.

[1] Abbreviations: TnC, troponin C; CTnC, troponin C C-domain; NMR, nuclear magnetic resonance; ΔV_f, volume change of folding; ΔG_f, free energy of folding.

10.1021/bi702058t CCC: $40.75
Published on Web 04/08/2008

Table 1: ΔV of Folding for the F105W/C-Domain and F105W/TnC in the Apo, Mg^{2+}-, or Ca^{2+}-Bound States

	2.1 mM $CaCl_2$			44 mM $MgCl_2$		EGTA	
urea M	F105W/C-domain ΔV mL/mol	F105W ΔV mL/mol	urea M	F105W/C-domain ΔV mL/mol	F105W ΔV mL/mol	F105W/C-domain ΔV mL/mol	F105W ΔV mL/mol
4.0	44.24 ± 2.88	39.97 ± 1.82	0.5	25.39 ± 0.89	24.34 ± 0.09	**27.71 ± 2.43** **32.5 ± 4.6 (NMR)**	**29.68 ± 0.26**
5.0	44.16 ± 0.58	46.57 ± 2.06	1.0	35.46 ± 1.39	33.86 ± 1.45		
6.0	51.27 ± 0.66	57.84 ± 2.70	1.5	34.31 ± 1.31	37.84 ± 2.43		
7.0	58.79 ± 0.45	**57.43 ± 1.56**	2.0	**35.61 ± 1.02**	**36.46 ± 1.75**		
8.0	**61.47 ± 1.75**						

filled N-domain resembles that of the C-domain, Herzberg et al. (*17*) proposed a model for the conformational changes that occur upon Ca^{2+}binding. This model postulates an opening of the N-domain that exposes its hydrophobic core, believed to be the site for attachment to the C-domain of TnI (*18–20*). Several lines of evidence have reinforced this model (*19, 21–28*) and recently, NMR and crystal structures of the N-domain filled by Ca^{2+} have corroborated the essential features of the model (*10, 20, 29–34*).

However, the C-domain interacts with the N-terminal of TnI (residues 1–47), attaching TnC to the troponin complex (for review see ref *3*). The structure of the calcium-saturated C-domain of skeletal TnC in complex with a regulatory peptide comprising residues 1–40 of TnI was determined using NMR spectroscopy (*35*). It is similar to the crystal structure of intact TnC in complex with the N-terminal fragment of TnI (*36*). In both cases, the structure of TnC free is less compact than the structure of TnC in complex with TnI. As a result, the TnC has a compact globular shape with direct interactions between the N- and C-terminal domains, in contrast to the elongated dumb-bell shaped molecule of uncomplexed TnC.

Fluorescence spectroscopy has been used extensively in studies of protein folding to determine changes in the tertiary and quaternary structures of proteins (*37*). Chicken skeletal muscle TnC is devoid of Trp or Tyr in its primary sequence. However, by site-directed mutagenesis, it is possible to replace different Phe residues by Trp with very little alteration of the natural properties in the mutant proteins (*38–41*). These mutants are suitable for fluorescence studies since there are marked alterations in the Trp fluorescence spectra as a result of the conformational changes that occur upon ion binding to nearby sites. In a recent report, Moncrieffe et al. (*41*) used two single tryptophan mutants (F78W and F154W) and observed the effects of metal ion binding on the optical spectroscopic properties and temperature stability of chicken skeletal TnC. The fluorescence emission and near-UV CD of W78 data showed that the N-terminal domain is sensitive to calcium binding at the C-terminal domain sites. They also observed that the N-terminal domain affects the stability of the C-terminal domain and vice versa. The results obtained by this group strongly suggested that there are interactions between the N- and C-terminal domains of TnC, even in the absence of TnI.

Here, we utilized a Trp mutant of the isolated C-domain (F105W/C-domain, residues 88–162) as well as the intact TnC with the same mutation (F105W). Position 105 faces site III in the C-domain (*39, 42*), and W105 serves as a probe for conformational changes in this region of the protein. Control experiments comparing the isolated N- and C-domain mutants with the intact protein show that the fluorescent signals from W29 and W105 faithfully report events in the N- and C-domains, respectively, uncontaminated by cross-talk from the other end of the molecule (*42*). Thus, the F105W mutation is ideally suited to an examination of the stability of the isolated C-domain in comparison with the intact protein and allows us to evaluate the contribution of the N-domain to the stability of the C-domain. The use of high pressure to induce dissociation and denaturation of proteins and biological assemblages is now widespread, and important thermodynamic parameters can be assessed by the use of this technique (*43–47*). However, the complete unfolding of monomeric proteins is generally achieved only at extremely high pressure (5–10 kbar; *45, 48, 49*), not attainable with common laboratory equipment. To overcome this limitation, the combination of high pressure with other perturbing agents, such as low temperature or subdenaturing concentrations of urea, has been employed (*27, 50–53*).

We find that the C-domain apo state seems to be completely denatured by pressure (in the range of 1–1000 bar) in the absence of urea as followed by changes in Trp emission and in NMR. Addition of Ca^{2+} or Mg^{2+} increased the C-domain stability so that complete denaturation was attained only by the combined use of high hydrostatic pressure and subdenaturing concentrations of urea, as determined by fluorescence and NMR spectroscopy. This combination allowed us to calculate the thermodynamic parameters (ΔV and ΔG°_{atm}) for folding of the C-domain in the presence of Ca^{2+} or Mg^{2+}. On analyzing the thermodynamic cycle for the folding of the isolated C-domain of TnC, taking into account all occupancy states, we conclude that the increase in stability of the C-domain when Ca^{2+} binds to it is almost twice the gain afforded by Ca^{2+} binding to the N-domain. Since the Ca^{2+} affinity of sites III and IV is 2 orders of magnitude higher than the affinity of sites I and II, we infer that part of this higher affinity of the C-domain for Ca^{2+} is contributed by the free-energy change of folding for this domain that takes place when Ca^{2+} binds.

MATERIAL AND METHODS

Reagents. All reagents were of analytical grade. Distilled water was filtered and deionized through a Millipore water purification system. Urea (ultrapure grade) was purchased from Sigma Chemical Co (St. Louis, MO).

Protein Preparation. A Trp was introduced into the cDNA of recombinant wild-type chicken TnC by site-directed mutagenesis, replacing Phe at position 105. The designation

Table 2: Experimental Free Energy Change and Volume Change Associated with Local Pressure-Induced Perturbations of Selected Peaks in Ca^{2+}-Saturated Wild-Type and F105W Mutant CTnC in the Presence of 4 M Urea-d_4 at 25 °C[a]

peak	Ca^{2+}-saturated wild-type CTnC		Ca^{2+}-saturated F105W CTnC	
	ΔG_f (kcal/mol)	ΔV_f (mL/mol)	ΔG_f (kcal/mol)	ΔV_f (mL/mol)
H128ϵ'	-0.89 ± 0.01	8.0 ± 0.7 (4.5)[b]	-0.6 ± 0.1	10 ± 1 (4.1)
W105ϵ3	N.A.	N.A.	N.A.	21.1 ± 0.8 (6.1)
F102ϵ and F112δ	-2.8 ± 0.2	26 ± 1 (4.6)	-3.2 ± 0.1	unresolved
F151δ	-2.9 ± 0.3	28 ± 3 (4.5)	-3.2 ± 0.3	32 ± 3 (4.4)
F102δ	-4.49 ± 0.06	41.7 ± 0.5 (4.4)	-4.1 ± 0.4	40 ± 4 (4.5)
β-sheet: F112α, I113α, I149α, D150α	-2.8 ± 0.3	37 ± 3 (4.1)	-5.8 ± 0.4	54 ± 4 (4.6)

[a] The samples were prepared in a buffered solution with +99% D_2O at pH* 7.00 ± 0.05. The pressure was varied from 1 bar to approximately 7.5 kbar. Complete denaturation of both proteins occurred by 6.7 kbar, as monitored by ^1H NMR at 300 MHz. [b] The pressure (in kbar) at 50% denaturation for each proton peak (determined by relative peak area as described in the text) is given in parentheses.

Table 3: ΔG of Folding for the F105W/C-Domain and F105W/TnC in the Apo, Mg^{2+}-, or Ca^{2+}-Bound States

	$\Delta G°$ kcal/mol (1241 bar)		$\Delta G°$ kcal/mol (1 bar)	
	F105W/C-domain	F105W	F105W/C-domain	F105W
EGTA			-0.42 ± 0.07 -0.54 ± 0.14 (NMR)	-0.44 ± 0.08
44 mM $MgCl_2$	-1.02 ± 0.10	-1.06 ± 0.13	-2.05 ± 0.13	-2.11 ± 0.18
2.1 mM $CaCl_2$	-2.79 ± 0.19	-2.78 ± 0.07	-4.56 ± 0.24	-4.44 ± 0.12

F105W/C-domain is for the fragment encompassing residues 88–162 of F105W. Proteins were expressed in *Escherichia coli* BL-21 cells and extracted and purified as previously described (*42*).

Hydrostatic Pressure. The experiments under pressure were performed at 20 °C in the standard buffer (100 mM Tris-HCl, 100 mM KCl, 1.0 mM DTT, and 1.5 mM EGTA, pH 7.0). Tris-HCl buffer was selected because the dependence of its pK_a on pressure is small. At 3.0 kbar, the value of pK_a increases by only 0.1 unit (*54*). The high-pressure cell has been described elsewhere (*55*). Temperature control was achieved through the use of a circulating water bath.

Spectroscopic Measurements. The Trp fluorescence spectra were recorded on an ISSK2 spectrofluorometer (ISS Inc., Champaign, IL). Samples were excited at 280 nm, and the emission was collected from 300 to 400 nm. Tryptophan fluorescence spectra at pressure p or in the presence of any concentration of urea u were quantified as the center of spectral mass $\nu_{p,u}$, in cm^{-1}:

$$\nu_{p,u} = \Sigma \nu_i Fi / Fi \quad (1)$$

where Fi stands for the fluorescence emitted at wavenumber ν_i, and the summation is carried out over the range of appreciable values of F.

The degree of denaturation (α) in a given condition was calculated from the changes in the center of spectral mass (ν) in that condition by

$$\alpha = (\nu_i - \nu)/(\nu_i - \nu_f) \quad (2)$$

where ν_i is the initial value of the center of spectral mass (native protein), and ν_f is the final value (unfolded protein). Spectra were recorded after 5 min of equilibration at each pressure. For the urea denaturation curves, the samples were incubated for 1 h in each concentration of urea. The protein concentration was 5 μM in all measurements. All spectroscopic changes reported were completely reversible.

Thermodynamic Parameters. The Gibbs free energy and the equilibrium constant for a given reaction depend on the standard volume change of the reaction (ΔV) according to the following relationship:

$$K_f(p) = K_{atm} \exp(p\Delta V/RT) \quad (3)$$

where $K_f(p)$ and K_{atm} are the equilibrium constants of folding at pressure p and atmospheric pressure, respectively. If we introduce the extent of reaction at pressure p, α_p, we deduce the following thermodynamic relationship (*55, 56*):

$$\ln(\alpha_p/(1-\alpha_p)) = p(\Delta V/RT) + \ln K_{atm} \quad (4)$$

For apo forms, we used eq 4 to determine the ΔV and K_{atm} values. In the presence of Ca^{2+} or Mg^{2+}, pressure alone was not enough to promote a complete unfolding. In these cases, the experiments were performed in the presence of increasing concentrations of urea. However, the volume change (ΔV) increased linearly with urea addition, leveling off at the highest concentration of urea used (Tables 1 and 3). This kind of behavior makes the use of the direct relationship between ΔG and the unfolding constant (K_{atm}) inappropriate. Thus, we first determined the free-energy change at 1241 bar in the presence of different concentrations of urea (eq 5). The extrapolation of this plot to 0 M urea gives $\Delta G^{\circ 0}M_{1241}$. This value was introduced into eq 6 to determine the free-energy change at atmospheric pressure ($\Delta G°_{atm}$).

$$\Delta G^{[U]}_{1241}{}^\circ = m[U] + \Delta G^{0M}_{1241}{}^\circ \quad (5)$$

$$\Delta G^{0M}_{1241}{}^\circ = \Delta G_{atm}{}^\circ + p\Delta V \quad (6)$$

where $\Delta G^{[U]}{}_{1241}°$ and $\Delta G^{0M}{}_{1241}°$ represent the free-energy change at 1241 bar in the presence or absence of urea, respectively, and m is the difference in solvent-accessible surface area as the protein unfolds (*31*). The volume change used in eq 6 was the highest value observed (marked in bold in Table 1). We chose 1241 bar because this pressure is close to the p_{50} values of the majority of the curves. In all experiments, after pressure release the spectroscopic changes were reversible.

NMR under Pressure. NMR assignments for the Ca^{2+}-saturated wild-type and F105W mutant fragments were obtained by 1D and 2D ^1H NMR experiments. The samples were prepared in the buffers previously described in both

+99% D_2O and 90%:10% H_2O:D_2O. Four hundred and 500 MHz ^{1}H NMR spectra were collected on Varian (Palo Alto, CA) systems equipped with commercial probes.

Variable high-pressure experiments were performed at proton Larmor frequencies of 300 MHz using high-pressure instrumentation, which has been described previously (*57*). The F105W/C-domain was dissolved in a pH 7.0 ± 0.05 buffer composed of 20 mM Tris-*d11*, 5 mM DTT, 2 mM EGTA, 100 mM KCl, and 1.5 mM TSP in D_2O.

At 300 MHz, 1D PRESAT experiments were typically performed at 25 °C with a 90° pulse width, up to a 4000 Hz sweep width, 16k complex points, a 6.5 s total delay between scans (1.25 s of a CW presaturation pulse) and 1024 scans. The measurements were taken at approximately 500-bar increments. The 300 MHz data were acquired with Mac NMR software (Tecmag Inc., Houston, TX) and were later processed with NUTS software (AcornNMR, Fremont, CA) using 3.0 Hz Gaussian and −3.0 Hz exponential multiplication.

Ca^{2+}-saturated wild-type and F105W mutant C-domain samples were prepared with a concentration of 0.7 mM in the +99% D_2O buffered solution described above, in the absence and presence of 4 M urea-d_4. Peak areas were obtained by using either a peak fitting routine or an integral routine in NUTS. The ^{1}H NMR data was processed and fitted three independent times to obtain error bars for our measurements. The peak areas in each spectrum were normalized to the TSP standard peak. The normalized peak areas at standard conditions (atmospheric pressure, 25 °C, and no urea) were assumed to describe the native state of the protein. To monitor the pressure denaturation of each peak, the normalized peak area at perturbed conditions (high pressures and/or presence of urea) was represented as a fraction of the native peak area (% native) as follows:

$$\%\ \text{Native} = \frac{\text{Normalized peak area at pressure P}}{\text{Normalized peak area at standard conditions}} = \frac{\text{Peak area at perturbed conditions}}{\text{TSP area at perturbed conditions}} \Big/ \frac{\text{Peak area at standard conditions}}{\text{TSP area at standard conditions}} \quad (7)$$

Assuming a 2-step equilibrium between the native and denatured states of the protein, the equilibrium constant and free energy of folding under given conditions (pressure, temperature, and urea) are represented by eqs 3 and 4. To calculate the change in volume (ΔV_u) of denaturation and therefore the value of folding ($\Delta V_f = -\Delta V_u$) for selected peaks, the natural logarithm of the equilibrium constant (ln K_{eq}) was plotted versus pressure. ΔV_u was calculated from the slope of this plot as follows:

$$\Delta V_u = -RT\frac{d(\ln K_{eq})}{dP} \quad (8)$$

RESULTS

Spectroscopic Properties of F105W/C-Domain and F105W in Different Occupancy States. Figure 1 shows the normalized intrinsic fluorescence spectra of F105W/C-domain in the absence and presence of divalent cations. In the apo form, the Trp mutant exhibits a red-shifted emission, indicating that the Trp is extremely exposed to the solvent. The center of spectral mass lies at 28,548 cm^{-1} (350 nm), a value close to the maximum observed for free Trp in solution (*37*). This suggests that this domain is almost devoid of tertiary contacts in the region around site III where the Trp is localized. However, upon Ca^{2+}binding a large blue shift of 630 cm^{-1} (approximately 8 nm) occurs (Figure 1). This displacement of the spectrum to the blue reflects the movement of Trp to the hydrophobic core of the protein. As shown in previous CD studies, this is accompanied by a concomitant increase in the helix content and in the compactness of the molecule (*42, 58, 59*). Similarly, the addition of 44.0 mM $MgCl_2$ displaces the Trp emission to blue by 300 cm^{-1}, which corresponds to 47% of the change induced by Ca^{2+}. A 10-fold increase in $MgCl_2$ concentration (to 440 mM) did not promote any further shift (not shown). These results suggest that the Trp residue faces different environments when Ca^{2+} fills sites III and IV than when Mg^{2+}fills them. In addition, the magnitude of the blue shift is proportional to the degree of solvent exposure and, thus, to the compactness of the folded structure. Therefore, in the Mg^{2+}-bound state, the Trp residue seems to be less buried than in the Ca^{2+}-bound form.

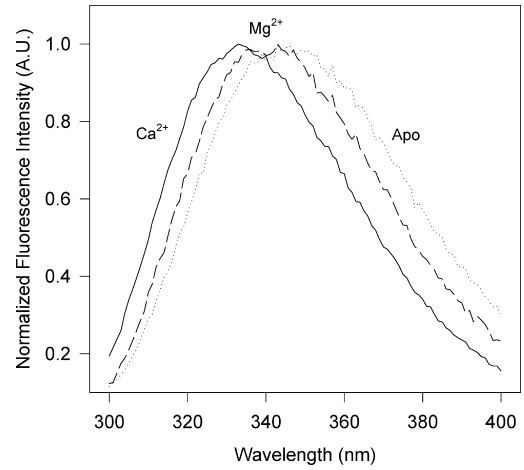

FIGURE 1: Normalized fluorescence emission spectra of F105W/C-domain in the absence of ions (•••) and in the presence of 44 mM $MgCl_2$ (---) or 2.1 mM $CaCl_2$ (—). The samples were excited at 280 nm and the emission measured from 300 to 400 nm. Protein concentration was 5 μM. The solvent conditions were 100 mM Tris-HCl at pH 7.0, 100 mM KCl, 1 mM DTT, and 1.5 mM EGTA at 20 °C.

Similar experiments were performed with intact TnC (F105W). Under all conditions, the center of spectral mass obtained with F105W resembled that observed for F105W/C-domain (cf. points at left in Figure 2). These findings are relevant because Ca^{2+} binding to F105W promotes only a very modest increase in the emission of Trp (*42*), which makes it difficult to extract structural information from fluorescence intensity changes.

Urea-Induced Denaturation of F105W/C-Domain and F105W. Figure 2 shows the changes in the center of spectral mass upon the addition of increasing concentrations of urea to F105W/C-domain (panel A) and to F105W (panel B). In the absence of divalent cations (triangles), very low concentrations of urea (2 M) were able to promote complete unfolding of the F105W/C-domain, with a shift in the center of spectral mass at 8 M urea to 28,400 cm^{-1}(352 nm). Strikingly, the center of spectral mass in the Ca^{2+}-bound form did not change significantly even in the presence of high concentrations of urea (Figure 2A, circles). These data confirm previous studies showing that Ca^{2+} binding markedly

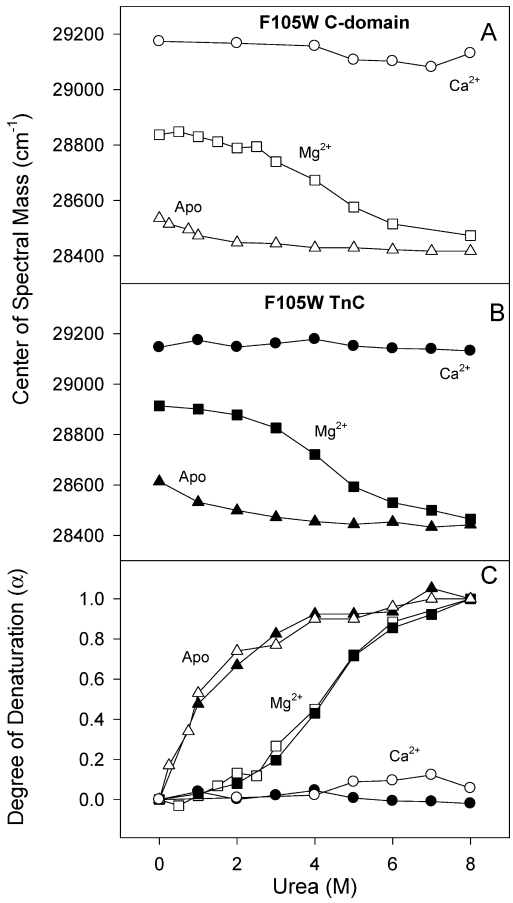

FIGURE 2: Changes in the center of spectral mass and unfolding as a function of [urea]. (A) F105W/C-domain; (B) F105W. In both panels, apo state, (△;▲); Mg^{2+}-bound state, (□;■); and Ca^{2+}-bound state, (●;○). (C) Degree of denaturation (α) as a function of [urea] for the data presented in panels A and B. Other conditions are as described in Figure 1.

stabilizes the structure of this domain (*60–63*). Thus, by using just urea as a denaturing agent, it is not possible to denature the isolated F105W/C-domain in the presence of Ca^{2+}. In the Mg^{2+}-bound state (squares), the F105W/C-domain exhibited an intermediate stability when compared to the apo or Ca^{2+}-bound forms, denaturing completely at 6 M urea (Figure 2A). Figure 2B shows the same stabilizing effects of Ca^{2+} and Mg^{2+} on the whole protein (F105W). For better comparison, the extent of unfolding (α, eq 2) as a function of urea concentration is shown in Figure 2C. In the apo or Mg^{2+}-bound state, the presence of the N-domain did not influence significantly the stability of the C-domain. Futhermore, the urea curves reveal that the W105 is unable to report the conformational change that occurs in the N-domain. In the presence of Ca^{2+}, both proteins were equally stable, and no denaturation was observed by measurements of Trp emission.

Pressure-Induced Denaturation of F105W/C-Domain and F105W as Detected by Fluorescence. Figure 3 shows the center of spectral mass as a function of pressure for the F105W/C-domain in the apo state and in the Mg^{2+}- and Ca^{2+}-bound states. In the absence of divalent cations, we observed a decrease in the center of spectral mass with an increase in pressure from 1 bar to 3.1 kbar, and the final value reached under high pressure is similar to that obtained by urea unfolding (see Figure 2A). Similar results

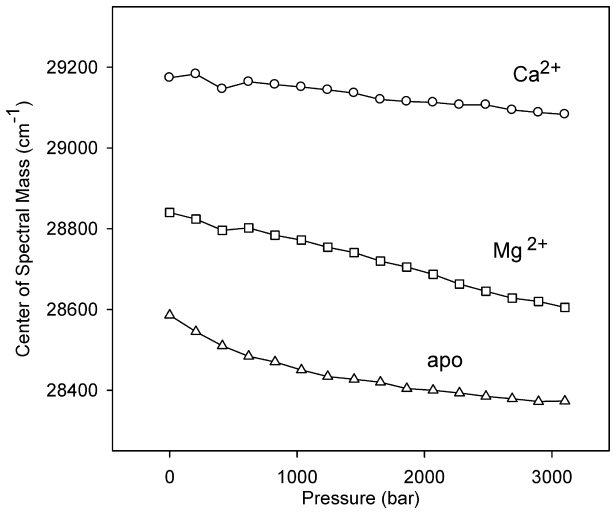

FIGURE 3: Effect of pressure on F105W/C-domain in the apo form (△), in the Mg^{2+}-bound form (□), and in the Ca^{2+}-bound form (○). F105W/C-domain was subjected to increasing pressure steps of 200 bar at 20 °C. Other conditions were the same as those described in Figure 1.

were attained with the intact protein (not shown). Since complete denaturation was achieved by pressure, it was possible to determine the volume change of folding for the apo form in the absence of urea (Table 1). These results suggest that pressure promotes extensive denaturation of the C-domain. However, in the presence of Mg^{2+}, the decrease in the center of spectral mass with an increase in pressure from 1 bar to 3.1 kbar is about 52% of that promoted by 8 M urea, indicating incomplete denaturation of the C-domain under pressure. Again, as observed in the urea unfolding experiment, binding of $Ca^{2+}$to the C-domain increases its thermodynamic stability, and only a small red shift (91 cm^{-1}) in the center of spectral mass is observed at 3.1 kbar.

Pressure-Induced Denaturation of Wild-Type C-Domain and F105W/C-Domain as Determined by NMR. The effect of pressure on the C-domain structure was also evaluated by ^{1}H NMR spectroscopy. As observed in Figure 4, the aromatic region of F105W/C-domain apo form appears to be perturbed by increasing pressure. The changes in the spectra include gradual downfield shifts of the peaks at ∼6.35 and 6.55 ppm and a broadening and loss of intensity in these peaks. The β-sheet resonances at 5.4 ppm also undergo broadening and decrease in intensity. The large cluster of peaks from 6.9 to 7.6 ppm merge together and simplify into two prominent peaks located at 7.2 and 7.35 ppm in the 3 kbar spectrum, suggesting that the protein may be collapsing toward a random-coil configuration. There is also a split of the His 128 signal in two peaks. We used the changes in the ratio of the two peaks of the histidine signal to evaluate the transition from the folded to the unfolded states. It resulted in a volume change of folding of 32.5 +/− 4.6 mL/mol and a folding free energy of –0.54 +/− 0.14 kcal/mol. This value is in good agreement with that obtained from the fluorescence experiments (Table 1). The lack of complete assignment of the structure of the apo form prevented us from analyzing the changes in the environment of other amino acid residues with pressure. The persistence of the upfield Phe resonances around 6.5 ppm and a residual intensity in the downfield

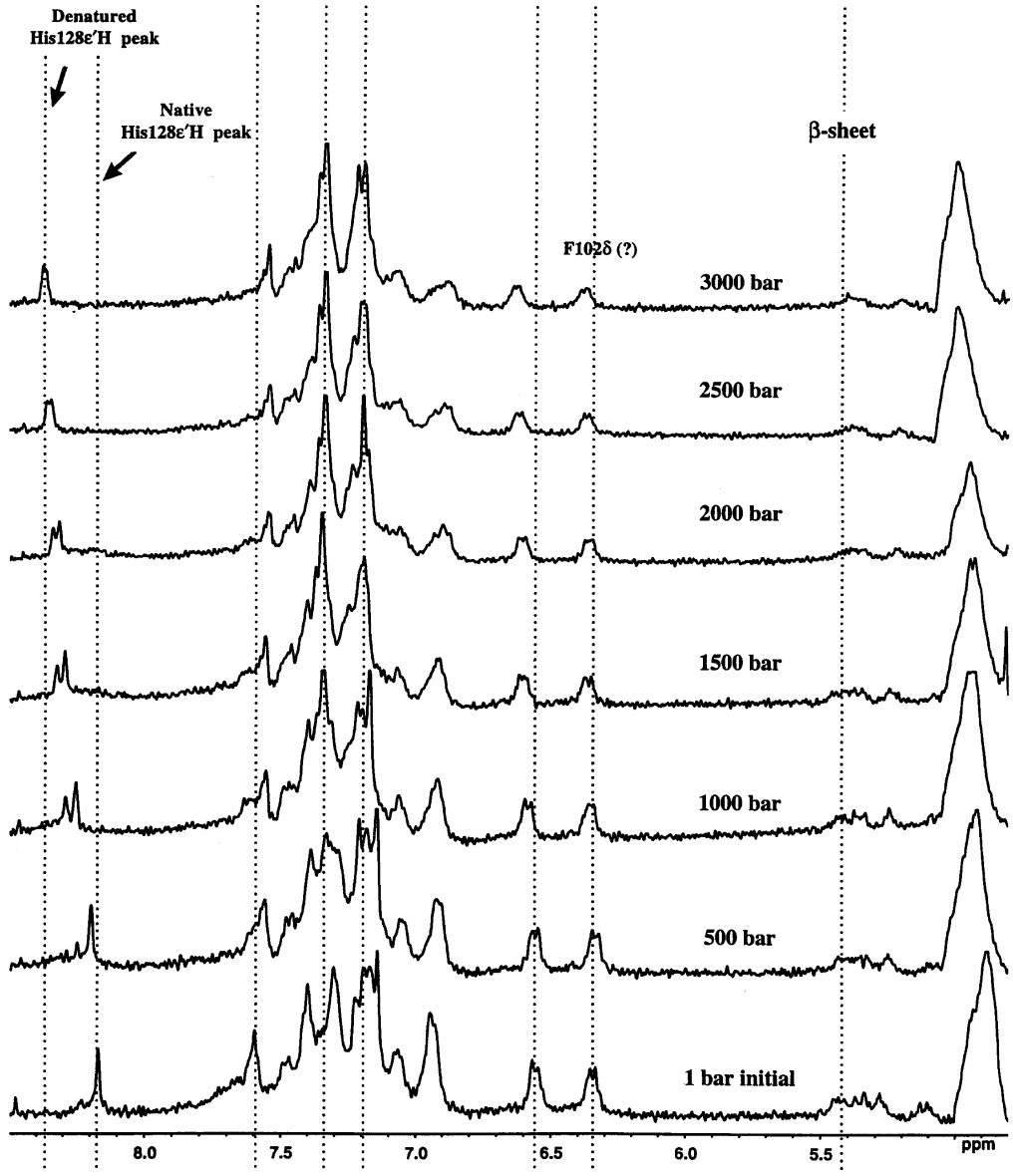

FIGURE 4: ^{1}H NMR spectra of the aromatic region of F105W/C-domain in the apo form. Pressure studies were performed on the 300 MHZ TecMag system with 1024 acquisitions, sw = 4000 Hz, 16k complex data points, and 25 °C. Spectra were processed using −3 Hz exponential multiplications, followed by 3 Hz Gaussian multiplication. Note that spectra are not drawn to scale.

β-sheet resonances at ~5.4 ppm suggest that the denatured protein has some residual structure.

The C-domain becomes so stable upon Ca^{2+} binding that high concentrations of urea or pressure alone were not enough to promote a complete red shift in the center of spectral mass of the protein (Figure 3). This behavior was confirmed by ^{1}H NMR (Supporting Information, Figure S1). In the presence of Ca^{2+}, few peaks from 6.9 to 7.6 ppm appear to be mobile with increasing pressure. In order to obtain proton assignments for the aromatic residues, ^{1}H−^{1}H TOCSY spectra were acquired at atmospheric pressure for the Ca^{2+}-saturated F105W CTnC sample at 40 °C and pH 7.00 ± 0.05. Our assignments of selected proton peaks in the Ca^{2+}-saturated F105W mutant CTnC fragment (residues 88–162) (Supporting Information, Table S1) agreed with published data for the intact chicken skeletal TnC molecule with 2 Ca^{2+} ions bound to the C-domain, in 15% TFE, pH 7.0, and 40 °C (*29*).

The Ca^{2+}-bound samples in the absence of chemical denaturants were found to be resistant to denaturation by high pressures. For both Ca^{2+}-saturated wild-type and F105W mutant CTnC fragments, pressure up to 5 kbar at 25 °C were unable to measurably disrupt the aromatic side chain region (Figure S1). Very little change in chemical shift or peak intensity was observed for the ^{1}H NMR signals due to H128ϵ', F151δ, F102δ, and the β-sheet protons for pressure up to 5 kbar at 25 °C. Spectral changes in the region spanning 7.1 to 7.7 ppm may be attributed to rearrangements of the aromatic residues at high pressures due to compression of the protein core.

The extreme persistence of structure in the Ca^{2+}-saturated wild-type and F105W mutant CTnC samples at high pressure required the use of more rigorous denaturing conditions. To assist the unfolding process, urea was added to destabilize the protein. The Ca^{2+}-saturated wild-type and the F105W mutant CTnC proteins were subjected to pressure as high as 7.5 kbar in the presence of 4 M urea-d_4 in +99% D_2O buffered solutions (Figure 5). Under these conditions, denaturation was achieved.

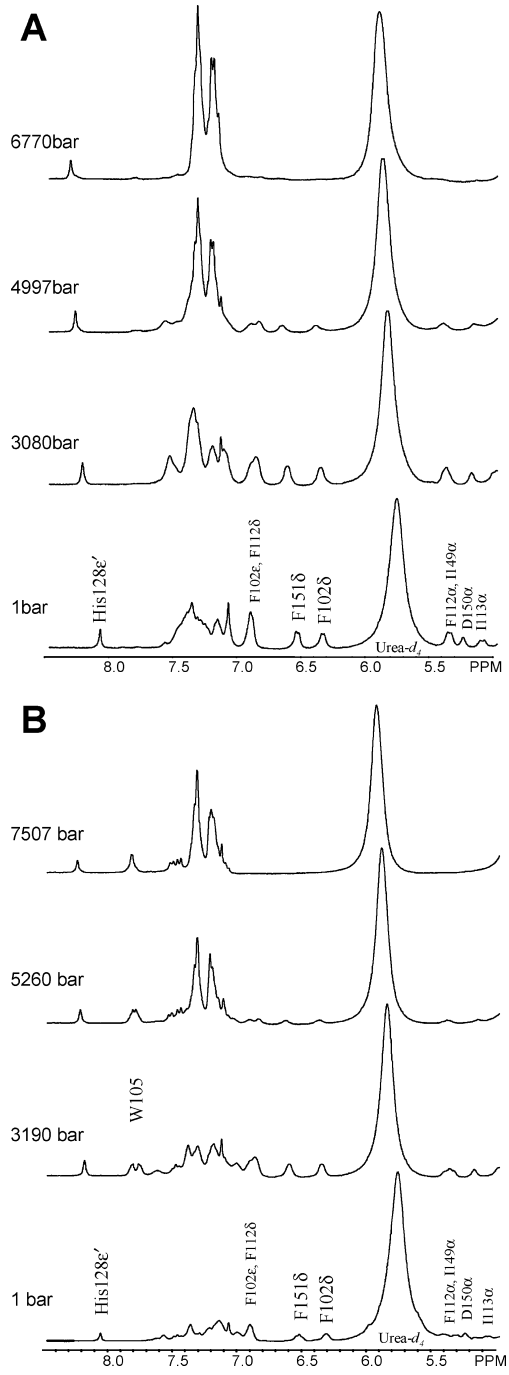

FIGURE 5: Selected 300 MHz ^{1}H NMR spectra of the Ca^{2+}-saturated (A) wild-type and (B) F105W mutant CTnC in the presence of 4 M Urea-d_4 at variable pressures at 25 °C. Samples contain 1 mM protein in a buffered 99+% D_2O solution described in the text at pH* 7.00 ± 0.05. The data was collected using a PRESAT pulse sequence, 1024 scans, 32K complex points, and 8000 Hz sweep width, and processed with 1 Hz exponential multiplication for reducing noise in NMR spectra (in the tail part of time-domain signals).

The change in volume (ΔV_f) upon folding is a physical parameter that can be extracted from pressure denaturation experiments and is proportional to the free energy change (ΔG_f) associated with the application of pressure to a system. The ΔV_u and ΔV_f for specific peaks can be directly calculated from the slope of a plot of ln K_{eq} versus P (Table 2, and Supporting Information, Figures S2 and S3). The values for ΔV were obtained for the following isolated peaks: H128ϵ' (8.3 ppm), W105ϵ3 (7.6 ppm), F151δ (6.6 ppm), and F102δ (6.4 ppm) based on the changes in the peak areas, as described in Materials and Methods (eq 7). Collective ΔV_f values for groups of protons with overlapping resonances were also calculated for F102ϵ and F112δ (both at 6.9 ppm) and for the β-sheet α-carbons F112α, I149 α, D150 α, and I113 α (ranging from 5.1 to 5.4 ppm) (Table 2). Note that no significant differences were observed for the ΔV_f values between the Ca^{2+}-saturated wild-type and F105W mutant proteins, suggesting that this mutation minimally perturbs the stability of these regions.

A large magnitude of ΔV_f for a particular region of a protein indicates that it undergoes a large change in volume upon denaturation (*64*). In our C-domain studies, the largest magnitudes for ΔG_f and ΔV_f were associated with the F102δ proton, which is located toward the center of the domain and with the β-sheet regions of the binding loops. Both of these regions participate in highly ordered structural elements. F102 is believed to be involved in hydrophobic ring-stacking interactions, while the β-sheet residues are held together by hydrogen bonds in an antiparallel arrangement (*65*). Interestingly, the F151δ and F105δ/W105ϵ3 protons, found on either side of F102, presented smaller magnitudes of ΔG_f and ΔV_f, suggesting that they are packed less tightly than the center. Therefore, the variations in ΔG_f and ΔV_f throughout the protein reveal how unfolding affects protein structure in a site-specific manner, which is uniquely dependent upon the stabilizing forces in the local environment of each residue. The values obtained for the amino acid sites located in the hydrophobic core are close to that obtained for the changes in the fluorescence of W105 (44 mL/mol; Tables 1 and 2) obtained under the same conditions (4 M urea). Generally, tryptophan fluorescence reflects the overall tertiary structure because its excited state samples the conformational space in a nanosecond window. Indeed, the similarity of the value of the volume change obtained by fluorescence to those values measured by NMR for residues that are closely packed in the hydrophobic core allowed us to use fluorescence to explore the pressure denaturation of CTnC at multiple concentrations of urea.

Thermodynamic Parameters of Folding of the F105W/C-Domain and F105W. As verified by NMR, the complete unfolding of the C-domain in the presence of cations was attained only when high pressure was combined with subdenaturing concentrations of urea. In Figure 6A and B, we monitored denaturation of the F105W/C-domain by measuring changes in the center of spectral mass of W105. As observed in each panel, different concentrations of urea were used to induce unfolding. In the Mg^{2+}-bound state, the concentration of urea necessary to promote complete denaturation was 2.0 M, while in the Ca^{2+}-bound state 7.0 or 8.0 M urea was required. For the pressure-induced denaturation of F105W, similar results were observed, and the addition of urea was also required in a concentration range very similar to those used with F105W/C-domain (data not shown). Note that the maximum red shift in the Trp emission observed when high pressure and urea were combined was similar to the shift promoted by the addition of urea at atmospheric pressure, in the absence of cations. This similarity indicates that both procedures can denature the protein to the same final state. The combination of pressure and urea has the advantage of allowing us to observe a complete unfolding curve in the presence of

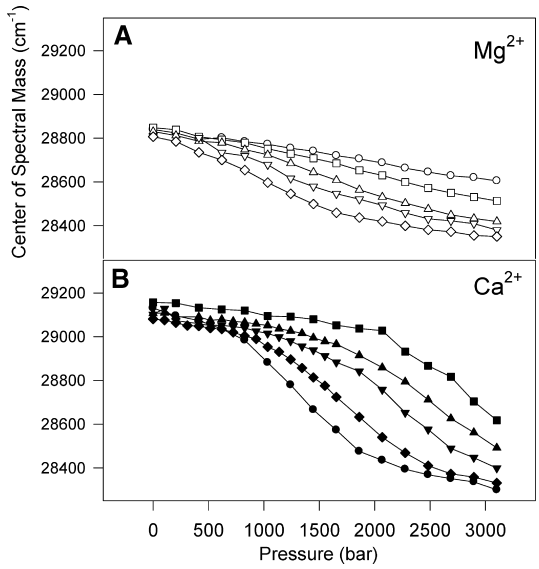

FIGURE 6: Pressure-induced denaturation of the F105W/C-domain in the presence of urea (A) in the Mg^{2+}-bound form and (B) in the Ca^{2+}-bound form. The concentrations of urea used in panel A were 0.5 M (□), 1 M (△), 1.5 M (▽), or 2 M urea (◊) and in panel B were 4 M (■), 5 M (▲), 6 M (▼), 7 M (♦), or 8 M urea (●). All other conditions were as described for Figure 1. Circles in panel A correspond to the condition in the absence of urea.

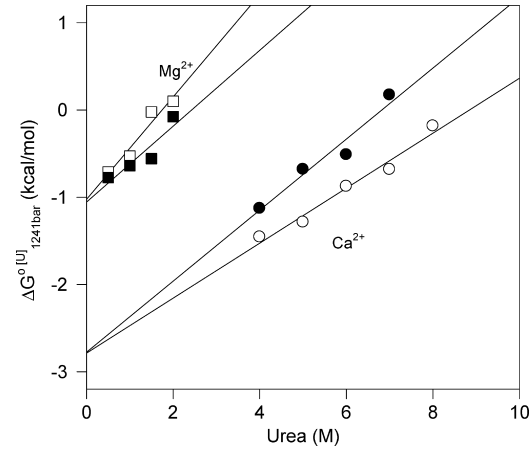

FIGURE 7: $\Delta G_{1241\ bar}$ at different concentrations of urea. From the pressure curves presented in Figure 6, $\Delta G_{1241bar}$ were calculated for the unfolding of F105W/C-domain (open symbols) or for F105W (filled symbols) in the presence of Ca^{2+} (circles) or Mg^{2+} (squares). Extrapolation of these curves to the *y*-axis gives $\Delta G_{1241bar}$ in the absence of urea.

Ca^{2+}. In previous reports, thermal denaturation was required to achieve this result (*60, 61, 63*).

From the pressure−denaturation curves, it was possible to calculate the volume change of folding for F105W/C-domain and F105W, under each condition (Table 1). In the apo form, ΔV was calculated from the pressure curve obtained in the absence of urea. In the presence of Mg^{2+} or Ca^{2+}, the volume change of folding increased with urea concentration until saturation was attained. The values reached at saturation are assumed to represent the equilibrium native ⇔ unfolded and are marked in bold in Table 1. Interestingly, in the apo, Mg^{2+}- and Ca^{2+}-bound states, we observed different values of volume change, probably a reflection of the differences in packing of the C-domain. It is also noteworthy that at the condition of 4 M urea the volume change derived from fluorescence is very similar to those derived from the changes in NMR signal of amino acid residues that are located in the hydrophobic core (Table 2), indicating that the fluorescence of tryptophan at position 105 is a good probe for the overall tertiary structure.

In other to calculate the $\Delta G_{atm}°$ for the folding process of apo forms, we used eq 4. In the presence of cations, we calculated the free energy at 1241 bar ($\Delta G^{0M}_{1241}°$) according to eq 5. Thus, we calculated the free-energy change at 1241 bar in the presence of different concentrations of urea as shown in Figure 7 for the isolated F105W/C-domain (open symbols) and F105W (filled symbols). Extrapolation of these curves to the *y*-axis furnishes $\Delta G°$ in the absence of urea at 1241 bar ($\Delta G^{0M}_{1241}°$). From eq 6, $\Delta G^{0M}_{1241}°$ leads to ΔG at atmospheric pressure in the absence of urea ($\Delta G_{atm}°$), as shown in Table 3. The free-energy change of folding for the C-domain apo form was very low, confirming its poor stability even in the intact protein (−0.4 kcal/mol). Upon Mg^{2+} binding, the stability of the isolated C-domain or in intact protein increased by ∼1.6 kcal/mol. In the presence of Ca^{2+}, the isolated C-domain and the intact protein show an increase in the stability of ∼4.0 kcal/mol. Considering that the $\Delta G_{atm}°$ values are identical, within error, whether or not the C-domain is attached to the N-domain, we conclude that there is no stabilizing or destabilizing effect of the N-domain on the C-domain structure. The fact that there is no effect on the overall stability does not exclude the possibility that the N-domain is making a contact with a segment of the protein in which W105 is not sensing. Our result corroborates the data of Tsalkova and Privalov (*61*), who observed that the destabilizing interaction between N- and C-domains decreases with an increase in the ionic strength.

DISCUSSION

Troponin C (TnC) is the Ca^{2+}-binding subunit of the troponin complex. It has two distinct domains, C and N, which show different properties, in spite of the high structural homology. In this article, we analyzed the thermodynamic stability of the C-domain of TnC, alone or in intact protein, using a fluorescent mutant with Phe 105 replaced by Trp. In the absence of cations, we observed that the W105 exhibits a red-shifted emission, indicating that the Trp is extremely exposed to the solvent. In fact, addition of 2 M urea promotes complete red shift in the Trp emission. Taken together these data suggest that the C-domain apo form has a partially folded conformation. Upon Ca^{2+} or Mg^{2+} binding, we observed a blue shift in Trp emission. This displacement of the spectrum to the blue region reflects the movement of Trp to the hydrophobic core of the protein and the compactness of structure. In the case of F105W and F105W/C-domain, the change in Trp emission is larger in the presence of Ca^{2+}. Addition of 44 mM $MgCl_2$ displaces the Trp emission to the blue region by 300 cm^{-1}, which corresponds to 47% of the change induced by Ca^{2+}. These results suggest that in the Mg^{2+}-bound state the Trp residue seems to be less buried than in the Ca^{2+}-bound form.

The unfolding curves shown in Figure 2 confirmed the low stability of the C-domain apo form and that binding of Ca^{2+} markedly stabilizes the structure of this domain. Interestingly, we also observed that the N-domain of TnC has practically no effect on the structure of the C-domain.

Moncrieffe et al. (*41*) observed a different behavior when they measured the temperature-dependent profiles of WT and TnC mutants by near-UV and far-UV CD. Using a fluorescent mutant with Phe 78 replaced by Trp, they observed that mutation has a destabilizing effect not only on the N-domain but also on the C-domain. Perhaps, in our case, the region around W105 is not affected by any conformational change that occurs in N-domain. In fact, the urea and pressure curves of F29W/N-domain and F29W (unpublished results) are completely different from the urea curves of F105W/C-domain (or F105W), especially in the absence of cations.

As demonstrated in Figure 3, high hydrostatic pressure induces a decrease in the center of spectral mass of the C-domain apo form, similar to that caused by urea. This result suggests that pressure shifts the equilibrium of the apo C-domain to the unfolded state. The complete unfolding of the C-domain in the presence of cations was attained only when high pressure was combined with subdenaturing concentrations of urea. From the pressure−denaturation curves, we calculated the ΔV and ΔG_{atm}° of folding for F105W/C-domain and F105W, in the absence and presence of Mg^{2+} and Ca^{2+}.

The high-pressure NMR experiments had the advantage over the fluorescence data because they allowed us to derive values of ΔV_f and ΔG_f for amino acid residues located in distinct regions of the protein structure (Table 2). High-pressure NMR has been successfully used to explore the protein conformation space from the bottom to the upper region of the folding funnel (*64*). Previous studies with other proteins employing both NMR and fluorescence have permitted the following of the changes in the tertiary structure as well as site-specific changes induced by pressure (*66, 67*). In a high-pressure study of the small oncogene product, p13(MTCP1), Kitahara et al. (*67*) found that the unfolding transition monitored by fluorescence was cooperative, whereas two kinds of NMR spectral changes were observed, depending on the pressure range. The changes in NMR below 2 kbar reflected an alternate conformer, whereas above this pressure, the NMR changes agreed with the fluorescence (*67*).

It would be expected that the greatest net change in volume would occur for regions that are very tightly packed in the folded protein, such as the hydrophobic core. The packing density within the interior core of a protein can be extremely efficient, approaching that observed in small organic crystals (*68*). Within the core, hydrophobic interactions are maximized, and these interactions are believed to be crucial for the proper folding and stabilization of the native state of a protein. Indeed, the largest ΔV_f values were found for residues located in the hydrophobic core (Table 2), and they resemble the values derived from the fluorescence experiments (Tables 1−3). Therefore, the thermodynamic values derived from the fluorescence experiment represent the average behavior of the tertiary conformation of the protein and can be used to compare the different states of the protein, as represented in Figure 8.

In Table 1, we show the ΔV of folding of F105W and F105W/C-domain. Three factors contribute to the magnitude of the volume change: release of electrostriction of charged and polar groups that become exposed to the solvent upon unfolding, elimination of packing defects and cavities, and the transfer of hydrophobic groups from the protein interior

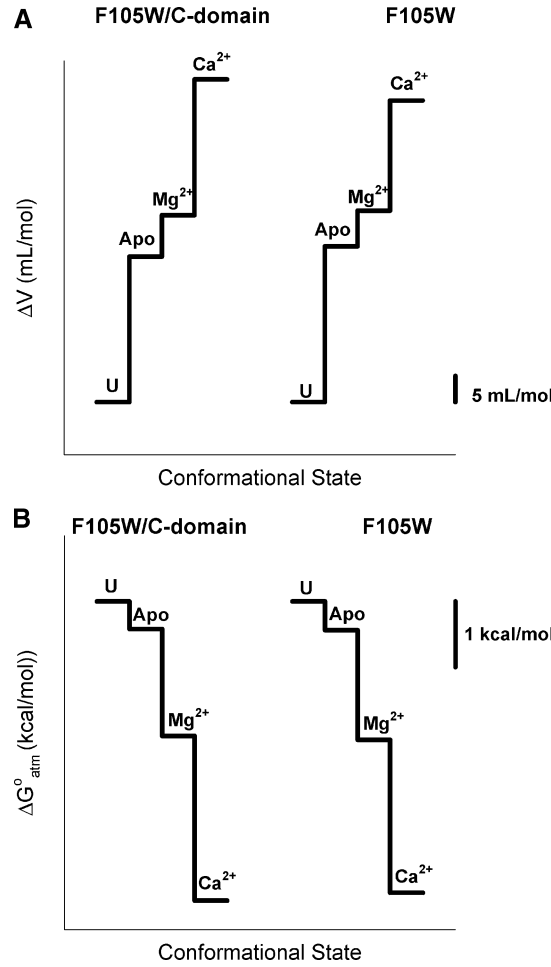

FIGURE 8: Thermodynamic diagrams for the folding of the F105W/C-domain and F105W. (A) Volume change. (B) Free-energy change at atmospheric pressure and 20 C.

to water (*47, 56, 69*). In the case of the C-domain, the apo form shows the smallest value for volume change of folding (27.7 mL/mol). This finding is compatible with the lack of organized structure, also evident in the fluorescence emission spectrum of W105 (red-shifted) and in the featureless CD spectrum (*42*). Furthermore, the presence of the N-domain had little effect on the organization of the C-domain: the calculated volume change for the intact protein was almost identical to that observed for the isolated C-domain (27.7 mL/mol and 29.8 mL/mol for the F105W/C-domain and F105W, respectively). We also observed that addition of Mg^{2+} to the F105W/C-domain caused only a modest increase in the volume change of folding. At first glance, this would appear to be inconsistent with the CD data, which show an increase in negativity that is almost as dramatic as that seen with Ca^{2+} (*41*). However, as pointed out by Mozhaev et al. (*69*), the breakage of hydrogen bonds that stabilize α helices is accompanied by rather small volume changes and, therefore, is not sensitive to pressure. This is due to the fact that breaking the hydrogen bonds between two amino acid residues in the folded state is replaced by the formation of hydrogen bonds between the amino acids and water, with no net change in volume. In addition, since the center of spectral mass is only partially shifted to the blue region when Mg^{2+} is bound (Figures 1 and 2), it is clear that additional rearrangements in the tertiary structure of this domain can still occur. It seems that the complete tertiary structural

organization of the C-domain is achieved only when Ca^{2+} is present, even though most, if not all, of the secondary structure forms when Mg^{2+} binds.

Calcium binding led to a pronounced increase in the volume change (61.5 mL/mol and 57.4 mL/mol for F105W/C-domain and F105W, respectively). As observed in the Mg^{2+}-bound state, the presence of the N-domain did not change the properties of the C-domain. Larger volume changes of folding would be expected for the intact protein because of the contribution of the N-domain. However, since W105 only reflects changes in the structure of the C-domain, the changes in the N-domain cannot be measured.

The solvent-excluded surface that appears with folding can be estimated from the volume change (*27, 70*). In the apo form, the volume change obtained experimentally as the protein folds (~ 28 mL/mol) corresponds to an increase in volume of 46.5Å^3 per molecule. Considering a nonpolar solvent as a model for calculating linear compressibility, this value corresponds to a solvent-excluded surface of 1024 Å^2 when the C-domain apo form folds. In the Mg^{2+}-bound form, this surface is 1280 Å^2, on the basis of a volume increase of 58.15 A^3. Thus, Mg^{2+} binding causes a net increase of ~12 A^3 in the volume of the system and 256 Å^2 in the solvent-excluded surface. Finally, the folding of the Ca^{2+}-bound form is accompanied by a much larger increase (2231 Å^2) and a volume increase of 101 Å^3. Thus, from apo to Mg^{2+}- and apo to Ca^{2+}-bound forms, the volume of C-domain increases by 12 ^{3} and 55 Å^3, respectively. These results can explain why intact myofibrils washed with EDTA (i.e., without any divalent cations) lose TnC from the thin filament much more rapidly than if Ca^{2+} or Mg^{2+} is present (*71, 72*).

The values of free-energy change of folding for the C-domain apo form derived from the fluorescence and NMR experiments coincide and were very low (Table 3), confirming its poor stability even in the intact protein (−0.4 kcal/mol). Our result is different from the one reported by Fredricksen and Swenson (*63*). However, the apo C-domain fragment (95–162) containing F102Y (apo-ChTnC95–162) showed no detectable transition due to the minimal amount of structure in the apo form (*63*). Therefore, the free-energy change of folding at 25 °C was obtained on the basis of Ca^{2+}-binding data. In our experiments, the pressure-induced unfolded produced a red shift in the emission of W105, and we were able to directly calculate the $\Delta G_{atm}°$ of folding of the C-domain.

The free-energy change of folding for the C-domain in the presence of Mg^{2+} or Ca^{2+} is also shown in Table 3. Binding of Mg^{2+} or Ca^{2+} induced an increase in protein stability. Here, the free-energy change of folding in our experiments is similar to that obtained by Fredricksen and Swenson (−2.4 kcal/mol for the Mg^{2+}-bound form and –3.6 kcal/mol for the Ca^{2+}-bound form). We also note that upon binding of Ca^{2+}, the stability of the C-domain increases approximately 10-fold, rendering the protein extremely stable against denaturation by various means (see also ref *63*). Nevertheless, it is interesting to note that the free-energy change of unfolding for the C-domain in the presence of Ca^{2+} is not very large (~4.5 kcal/mol), and, in fact, it is much lower than the free energy for the unfolding of several other proteins that undergo denaturation up to 8 M urea. Tsalkova and Privalov (*60*) have pointed out that TnC in the presence of Ca^{2+} exhibits the maximum number value of intrapeptide hydrogen bonds possible for a globular protein (0.7 bonds per residue), suggesting a plausible source of the stabilization forces conferred by Ca^{2+} binding.

Complete thermodynamic cycles for the folding of the C-domain alone and within the intact protein in all of its occupancy states are shown in Figure 8. These cycles summarize all of the results obtained using high pressure and subdenaturing concentrations of urea and also show that the C-domain structure, as reported by W105, is not affected by the presence of the N-domain. The cycle also shows how the tight coupling between calcium binding and troponin folding is driven by free energy.

ACKNOWLEDGMENT

We thank Professors Jiri Jonas and Ana Jonas for their insights and for the use of the high-pressure NMR equipment. We also thank Professor Lawrence B. Smillie and Joyce R. Pearlstone for donating the plasmids and for helpful suggestions. We are grateful to Emerson R. Gonçalves for competent technical assistance.

SUPPORTING INFORMATION AVAILABLE

Table S1 shows the assignments of selected proton peaks in the Ca^{2+}-saturated F105W mutant CTnC fragment (residues 88–162). Figure S1 depicts the effects of pressure on Ca^{2+}-saturated wild-type and F105W mutant CTnC fragments in the absence of urea. Figures S2 and S3 show the pressure dependence of the peak areas and the natural logarithm of the equilibrium constant (ln K_{eq}) for selected peaks in the ^{1}H NMR spectra of Ca^{2+}-saturated wild-type CTnC and F105W mutant CTnC, respectively, in the presence of 4 M urea. This material is available free of charge via the Internet at http://pubs.acs.org.

REFERENCES

1. Strynadka, N. C. J., and James, M. N. G. (1989) Crystal structures of the helix-loop-helix calcium-binding proteins. *Annu. Rev. Biochem. 58*, 951–998.
2. Falke, J. J., Drake, S. K., Hazard, A. L., and Peerse, O. B. (1994) Molecular tuning of ion binding to calcium signaling proteins. *Q. Rev. Biophys. 27*, 262–290.
3. Farah, C. S., and Reinach, F. C. (1995) The troponin complex and regulation of muscle contraction. *FASEB J. 9*, 755–767.
4. Tobacman, L. S. (1996) Thin filament-mediated regulation of cardiac contraction. *Annu. Rev. Physiol. 58*, 447–481.
5. Squire, J. M., and Morris, E. P. (1998) A new look at thin filament regulation in vertebrate skeletal muscle. *FASEB J. 12*, 761–771.
6. Gordon, A. M., Homsher, E., and Regnier, M. (2000) Regulation of contraction in striated muscle. *Physiol. Rev. 80*, 853–924.
7. Herzberg, O., and James, M. N. G. (1985) Structure of the calcium regulatory muscle protein troponin C at 2.8 Å resolution. *Nature 313*, 653–659.
8. Sundaralingam, M., Bergstrom, R., Strasburg, G., Rao, S. T., Roychowdhury, P., Greaser, M., and Wang, B. C. (1985) Molecular structure of troponin C from chicken skeletal muscle at 3-angstrom resolution. *Science 227*, 945–948.
9. Satyshur, K. A., Rao, S. T., Pyzalska, D., Drendel, W., Greaser, M., and Sundaralingam, M. (1988) Refined structure of chicken skeletal muscle troponin C in the two calcium state at 2 Å resolution. *J. Biol. Chem. 263*, 1628–1647.
10. Houdusse, A., Love, M. L., Dominguez, R., Grabarek, Z., and Cohen, C. (1997) Structures of four Ca^{2+}-bound troponin C at 2.0 Å resolution: further insights into the Ca^{2+}-switch in the calmodulin superfamily. *Structure 12*, 1695–1711.
11. Andersson, T., Drakenberg, T., Forsén, S., and Thulin, E. (1981) A 43 Ca NMR and ^{25}Mg NMR study of rabbit skeletal muscle troponin C: exchange rates and binding constants. *FEBS Lett. 1*, 39–43.

12. Hincke, M. T., McCubbin, W. D., and Kay, C. M. (1978) Calcium-binding properties of cardiac and skeletal troponin C as determined by circular dichroism and ultraviolet difference spectroscopy. *Can. J. Biochem. 6*, 384–395.
13. Johnson, J. D., Collins, J. H., Robertson, S. P., and Potter, J. D. (1980) A fluorescent probe study of Ca^{2+} binding to the Ca^{2+}-specific sites of cardiac troponin and troponin C. *J. Biol. Chem. 255*, 9635–9640.
14. Potter, J. D., and Gergely, J. (1975) The calcium and magnesium binding sites on troponin and their role in the regulation of myofibrillar adenosine triphosphatase. *J. Biol. Chem. 250*, 4628–4633.
15. Braga, C. A., Pinto, J. R., Valente, A. P., Silva, J. L., Sorenson, M. M., Foguel, D., and Suarez, M. C. (2006) Ca^{2+} and Mg^{2+} binding to weak sites of TnC C-domain induces exposure of a large hydrophobic surface that leads to loss of TnC from the thin filament. *Int. J. Biochem. Cell Biol. 38*, 110–122.
16. Grabarek, Z., Tao, T., and Gergely, J. (1992) Molecular mechanism of troponin C function. *J. Musc. Res. Cell Motil. 13*, 383–393.
17. Herzberg, O., Moult, J., and James, M. N. G. (1986) A model for the Ca^{2+}-induced conformational transition of troponin C. *J. Biol. Chem. 261*, 2683–2684.
18. Farah, C. S., Miyamoto, C. A., Ramos, C. H. I., da Silva, A. C. R., Quaggio, R. B., Fujimori, K., Smillie, L. B., and Reinach, F. C. (1994) Structural and regulatory functions of the NH2- and COOH-terminal regions of skeletal muscle troponin I. *J. Biol. Chem. 269*, 5230–5240.
19. Olah, G. A., and Trewhella, J. (1994) A model structure of the muscle protein complex $4Ca^{2+}$.troponin C.troponin I derived from small-angle scattering data: implications for regulation. *, Biochemistry 43*, 12800–12006.
20. McKay, R. T., Tripet, B. P., Hodges, R. S., and Sykes, B. D. (1997) Interaction of the second binding region of troponin I with the regulatory domain of skeletal muscle troponin C as determined by NMR spectroscopy. *J. Biol. Chem. 272*, 28494–28500.
21. Tao, T., Scheiner, C. J., and Lamkin, M. (1986) Site-specific photo-cross-linking studies on interactions between troponin and tropomyosin and between subunits of troponin. *Biochemistry 23*, 7633–7639.
22. Leszyk, J., Grabarek, Z., Gergely, J., and Collins, J. H. (1990) Characterization of zero-length cross-links between rabbit skeletal muscle troponin C and troponin I: evidence for direct interaction between the inhibitory region of troponin I and the NH_2-terminal, regulatory domain of troponin C. *Biochemistry 29*, 299–304.
23. Ngai, S. M., Sonnichsen, F. D., and Hodges, R. S. (1994) Photochemical cross-linking between native rabbit skeletal troponin C and benzoylbenzoyl-troponin I inhibitory peptide, residues 104–115. *J. Biol. Chem. 269*, 2165–2172.
24. Kobayashi, T., Grabarek, Z., Gergely, J., and Collins, J. H. (1995) Extensive interactions between troponins C and I. Zero-length cross-linking of troponin I and acetylated troponin C. *Biochemistry 29*, 10946–10952.
25. Pearlstone, J. R., and Smillie, L. B. (1995) Evidence for two-site binding of troponin I inhibitory peptides to the N and C domains of troponin C. *Biochemistry 34*, 6932–6940.
26. Jha, P. K., Leavis, P. C., and Sarkar, S. (1996) Interaction of deletion mutants of troponins I and T: COOH-terminal truncation of troponin T abolishes troponin I binding and reduces Ca2+ sensitivity of the reconstituted regulatory system. *Biochemistry 35*, 16573–16580.
27. Foguel, D., Suarez, M. C., Barbosa, C., Rodrigues, J. J., Sorenson, M. M., Smillie, L. B., and Silva, J. L. (1996) Mimicry of the calcium-induced conformational state of troponin C by low temperature under pressure. *Proc. Natl. Acad. Sci. U.S.A. 93*, 10642–10646.
28. Tripet, B., Van Eyk, J. E., and Hodges, R. S. (1997) Mapping of a second Actin-tropomyosin and a second troponin C binding site within the C terminus of troponin I, and their importance in the Ca^{2+}-dependent regulation of muscle contraction. *J. Mol. Biol. 271*, 728–750.
29. Slupsky, C. M., and Sykes, B. D. (1995) NMR solution structure of calcium-saturated skeletal muscle troponin C. *Biochemistry 34*, 15953–15964.
30. Gagné, M. S., Sakae, T., Li, M. X., Smillie, L. B., and Sykes, B. D. (1995) Structures of the troponin C regulatory domains in the apo and calcium-saturated states. *Nat. Struct. Biol. 2*, 784–789.
31. Strynadka, N. C., Cherney, M., Sielecki, A. R., Li, M. X., Smillie, L. B., and James, M. N. (1997) Structural details of a calcium-induced molecular switch: X-ray crystallographic analysis of the calcium-saturated N-terminal domain of troponin C at 1.75 Å resolution. *J. Mol. Biol. 273*, 238–255.
32. Mercier, P., Ferguson, R. E., Irving, M., Corrie, J. E., Trentham, D. R., and Sykes, B. D. (2003) NMR structure of a bifunctional rhodamine labeled N-domain of troponin C complexed with the regulatory "switch" peptide from troponin I: implications for in situ fluorescence studies in muscle fibers. *Biochemistry 42*, 4333–4348.
33. Takeda, S., Yamashita, A., Maeda, K., and Maeda, Y. (2003) Structure of the core domain of human cardiac troponin in the Ca(2+)-saturated form. *Nature 424*, 35–41.
34. Vinogradova, M. V., Stone, D. B., Malanina, G. G., Karatzaferi, C., Cooke, R., Mendelson, R. A., and Fletterick, R. J. (2005) Ca(2+)-regulated structural changes in troponin. *Proc. Natl. Acad. Sci. U.S.A. 102*, 5038–5043.
35. Mercier, P., Spyracopoulos, L., and Sykes, B. D. (2001) Structure, dynamics, and thermodynamics of the structural domain of troponin C in complex with the regulatory peptide 1–40 of troponin I. *Biochemistry 34*, 10063–10077.
36. Vassylyev, D. G., Takeda, S., Wakatsuki, S., Maeda, K., and Maeda, Y. (1998) Crystal structure of troponin C in complex with troponin I fragment at 2.3–Å resolution. *Proc. Natl. Acad. Sci. U.S.A. 95*, 4847–4852.
37. Lakowicz, J. R. (1999) *Principles of Fluorescence Spectroscopy*, 2nd ed., Springer Publishing, New York.
38. Pearlstone, J. R., Borgford, T., Chandra, M., Oikawa, K., Kay, C. M., Herzberg, O., Moult, J., Herklotz, A., Reinach, F. C., and Smillie, L. B. (1992) Construction and characterization of a spectral probe mutant of troponin C: application to analyses of mutants with increased Ca^{2+} affinity. *Biochemistry 28*, 6545–6553.
39. Trigo-Gonzalez, G., Racher, K., Burtnick, L., and Borgford, T. (1992) A comparative spectroscopic study of tryptophan probes engineered into high and low-affinity domains of recombinant chicken troponin C. *Biochemistry 31*, 7009–7015.
40. Chandra, M., da Silva, E. F., Sorenson, M. M., Ferro, J. A., Pearlstone, J. R., Nash, B. E., Borgford, T., Kay, C. M., and Smillie, L. B. (1994) The effects of N helix deletion and mutant F29W on the Ca2+ binding and functional properties of chicken skeletal muscle troponin. *J. Biol. Chem. 269*, 14988–14994.
41. Moncrieffe, M. C., Venyaminov, S. Y., Miller, T. E., Guzman, G., Potter, J. D., and Prendergast, F. G. (1999) Optical spectroscopic characterization of single tryptophan mutants of chicken skeletal troponin C: evidence for interdomain interaction. *Biochemistry 37*, 11973–11983.
42. Li, M. X., Chandra, M., Pearlstone, J. R., Racher, K. I., Gonzalez, G. T., Borgford, T., Kay, C. M., and Smillie, L. B. (1994) Properties of isolated recombinant N and C domains of chicken troponin C. *Biochemistry 33*, 917–925.
43. Silva, J. L., Foguel, D., Da Poian, A. T., and Prevelige, P. E. (1996) The use of hydrostatic pressure as a tool to study viruses and other macromolecular assemblages. *Curr. Opin. Struct. Biol. 6*, 166–175.
44. Panick, G., Vidugiris, G. J., Malessa, R., Rapp, G., Winter, R., and Royer, C. A. (1999) Exploring the temperature-pressure phase diagram of staphylococcal nuclease. *Biochemistry 13*, 4157–4164.
45. Silva, J. L., Foguel, D., and Royer, C. A. (2001) Pressure provides new insights into protein folding, dynamics and structure. *Trends Biochem. Sci. 26*, 612–618.
46. Foguel, D., and Silva, J. L. (2004) New insights into the mechanisms of protein misfolding and aggregation in amyloidogenic diseases derived from pressure studies. *Biochemistry 36*, 11361–11370.
47. Meersman, F., Dobson, C. M., and Heremans, K. (2006) Protein unfolding, amyloid fibril formation and configurational energy landscapes under high pressure conditions. *Chem. Soc. Rev. 10*, 908–917.
48. Brandts, J. F., Oliveira, R. J., and Westort, C. (1970) Thermodynamics of protein denaturation. Effect of pressure on the denaturation of ribonuclease A. *Biochemistry 9*, 1038–1047.
49. Zipp, A., and Kauzmann, W. (1973) Pressure denaturation of metmyoglobin. *Biochemistry 12*, 4217–4228.
50. Foguel, D., and Weber, G. (1995) Pressure-induced dissociation and denaturation of allophycocyanin at subzero temperatures. *J. Biol. Chem. 270*, 28759–28766.
51. Mohana-Borges, R., Silva, J. L., Ruiz-Sanz, J., and de Prat-Gay, G. (1999) Folding of a pressure-denatured model protein. *Proc. Natl. Acad. Sci. U.S.A. 14*, 7888–7893.

52. Lima, L. M., Foguel, D., and Silva, J. L. (2000) DNA tightens the dimeric DNA-binding domain of human papillomavirus E2 protein without changes in volume. *Proc. Natl. Acad. Sci. U.S.A. 9*, 14289–14294.
53. Suarez, M. C., Machado, C. J. V., Lima, L. M. T. R., Smillie, L. B., Pearlstone, J. R., Silva, J. L., Sorenson, M. M., and Foguel, D. (2003) Role of hydration in the closed-to-open transition involved in Ca2+ binding by troponin C. *Biochemistry 42*, 5522–5530.
54. Neuman, R. C., Kauzmann, W., and Zipp, A. (1973) *J. Phys. Chem. 77*, 2687–2691.
55. Paladini, A. A., and Weber, G. (1981) Pressure-induced reversible dissociation of enolase. *Biochemistry 20*, 2587–2593.
56. Silva, J., and Weber, G. (1993) Pressure stability of proteins. *Annu. Rev. Phys. Chem. 44*, 89–113.
57. Jonas, J., Koziol, P., Peng, X., Reiner, C., and Campbell, D. M. (1993) *J. Magn. Reson. B 102*, 299.
58. Murray, A. C., and Kay, C. M. (1972) Hydrodynamic and optical properties of troponin. Demonstration of conformational change upon binding calcium ion. *Biochemistry 11*, 2622–2627.
59. Van Eerd, J. P., and Kawasaki, Y. (1972) Ca++ induced conformational changes in the Ca++ binding component of troponin. *Biochem. Biophys. Res. Commun. 47*, 859–864.
60. Tsalkova, T. N., and Privalov, P. L. (1980) Stability of troponin C. *Biochim. Biophys. Acta 624*, 196–204.
61. Tsalkova, T. N., and Privalov, P. L. (1985) Thermodynamic study of domain organization in troponin C and calmodulin. *J. Mol. Biol. 181*, 533–544.
62. Brzeska, H., Venyaminov, S. V., Grabarek, Z., and Drabikowski, W. (1983) Comparative studies on thermostability of calmodulin, skeletal muscle troponin C and their tryptic fragments. *FEBS Lett. 153*, 169–173.
63. Fredricksen, R. S., and Swenson, C. A. (1996) Relationship between stability and function for isolated domains of troponin C. *Biochemistry 35*, 14012–14026.
64. Lassalle, M. W., and Akasaka, K. (2007) The use of high-pressure nuclear magnetic resonance to study protein folding. *Methods Mol. Biol. 350*, 21–38.
65. Slupsky, C. M., Reinach, F. C., Smillie, L. B., and Sykes, B. D. (1995) Solution secondary structure of calcium-saturated troponin C monomer determined by multidimensional heteronuclear NMR spectroscopy. *Protein Sci. 4*, 1279–1290.
66. Peng, X., Jonas, J., and Silva, J. L. (1993) Molten-globule conformation of Arc repressor monomers determined by high-pressure 1H NMR spectroscopy. *Proc. Natl. Acad. Sci. U.S.A. 90*, 1776–1780.
67. Kitahara, R., Royer, C., Yamada, H., Boyer, M., Saldana, J. L., Akasaka, K., and Roumestand, C. (2002) Equilibrium and pressure-jump relaxation studies of the conformational transitions of P13MTCP1. *J. Mol. Biol. 320*, 609–628.
68. Richards, F. M. (1974) The interpretation of protein structures: total volume, group volume distributions and packing density. *J. Mol. Biol. 82*, 1–14.
69. Mozhaev, V. V., Heremans, K., Frank, J., Masson, P., and Balny, C. (1996) High pressure effects on protein structure and function. *Proteins 24*, 81–91.
70. Foguel, D., Silva, J. L., and de Prat-Gay, G. (1998) Characterization of a partially folded monomer of the DNA-binding domain of human papillomavirus E2 protein obtained at high pressure. *J. Biol. Chem. 15*, 9050–9057.
71. Sorenson, M. M., Silva, A. C. R., Gouveia, C. S., Sousa, V. P., Oshima, W., Ferro, J. A., and Reinach, F. C. (1995) Concerted action of the high affinity calcium binding sites in skeletal muscle troponin C. *J. Biol. Chem. 270*, 9770–9777.
72. Sousa, V. P., Pinto, J. R., and Sorenson, M. M. (2006) Ionic interventions that alter the association of troponin C C-domain with the thin filaments of vertebrate striated muscle. *Biochim. Biophys. Acta 2*, 272–282.

BI702058T